

The Assessment of Dispersion of Fine Ceramic Powders for Injection Moulding and Related Processes

J. H. Song & J. R. G. Evans

Department of Materials Technology, Brunel University, Uxbridge, Middlesex UB8 3PH, UK

(Received 2 February 1993; revised version received 23 April 1993; accepted 15 June 1993)

Abstract

A method for the assessment of dispersion of fine ceramic powders in an organic vehicle for use in injection moulding and related processes is described. The procedure combines the quantitative evaluation of maximum shear stress in twin-roll mixing with the examination of agglomerate breakdown by scanning electron microscopy using the back-scattered electron image technique. The effect of shear stress, mixing time and the strength of agglomerates on the dispersive mixing process was investigated. Two spray-dried ZrO₂ powders and one TiO₂ powder were examined by mixing with a polystyrene vehicle. The results suggest that the maximum shear stress during mixing should be five to 10 times greater than the agglomerate strength in order to disperse the powder in an organic vehicle. Mixing time was found to be less important. The microscopical technique can be used on its own to examine the state of dispersion of powders in organic materials after dilution in the mixing device.

Eine Methode zur Einschätzung der Dispersion von feinen Keramikpulvern in einem organischen Träger wird beschrieben. Diese Dispersionen werden beim Spritzgießen und ähnlichen Verfahren verwendet. Das Verfahren verbindet die quantitative Berechnung der maximalen Scherspannung beim Zwillingswalzen, Mahlen und Mischen mit der elektronenmikroskopischen Untersuchung des Zerbrechens des Agglomerats unter Verwendung von rückgestreuten Elektronen. Der Einfluß der Scherspannung, der Mischzeit und der Festigkeit des Agglomerats auf den dispersiven Mischprozeß wurde untersucht. Zwei sprühgetrocknete ZrO₂-Pulver und ein TiO₂-Pulver wurden mit einem Polystyrenträger gemischt und untersucht. Aus den Ergebnissen läßt sich schließen, daß die maximale Scherspannung während des

Mischens mindestens 5–10 mal größer sein sollte als die Festigkeit des Agglomerats, um das Pulver im organischen Träger zu verteilen. Es hat sich gezeigt, daß die Mischzeit keinen großen Einfluß hat. Die Mikroskopietechnik kann auch alleine verwendet werden, um den Dispersionszustand des Pulvers in einem organischen Material nach der Verdünnung in einem Mischer zu untersuchen.

On décrit une méthode permettant d'évaluer la dispersion de poudres céramiques techniques dans un milieu organique, destinée au moulage par injection et aux procédés connexes. La procédure utilisée combine l'évaluation quantitative de la contrainte de cisaillement maximale, effectuée dans un broyeur-mélangeur à rouleaux, avec l'examen de la rupture des agglomérats par microscopie électronique à balayage, en utilisant la technique des images d'électrons rétrodiffusés. On a examiné l'effet de la contrainte de cisaillement, de la durée du mélange et la résistance des agglomérats sur le procédé de mélange dispersif. Des poudres de ZrO₂ séchées par atomisation et une poudre de TiO₂ ont fait l'objet d'un examen lors du mélange dans un milieu polystyrène. Les résultats suggèrent que la contrainte de cisaillement maximale durant le mélange devrait être au moins 5–10 fois plus grande que la résistance des agglomérats pour pouvoir disperser la poudre dans un milieu organique. La durée de broyage est moins importante. La technique microscopique peut être utilisée pour elle-même afin d'examiner l'état de dispersion des poudres dans des matériaux inorganiques après dilution dans l'appareil de mélange.

1 Introduction

Agglomeration occurs naturally in ceramic powders because of adhesion forces between fine particles.¹

Agglomerates are sometimes intentionally formed to meet the special needs of powder processing. For example, spray-drying is widely used to form spherical agglomerates to improve the flow properties in compaction of ceramic powders. In ceramic injection moulding and related processes, however, agglomeration is neither necessary nor desirable. Agglomerates should be broken down by intensive shear compounding so as to reduce the agglomerate size to an acceptable level dictated by the preferred maximum defect size in the fired body. This is known as dispersive mixing. It should be accompanied by the uniform distribution of dispersed particles throughout the organic vehicle (distributive mixing). These goals rest upon the thesis that residual undispersed agglomerates may cause strength-limiting defects in the final sintered products.^{2,3}

Among the perceived advantages of injection moulding and related processes are the lack of reliance on a powder which is handicapped by deliberate agglomeration and the ability of shear mixing processes to destroy natural agglomerates at an early stage. Nevertheless, due to the limitation on the shear stress which can be set up in the suspension by the mixing machinery, the ceramic powder and the mixing conditions need to be carefully selected. This requires an experimental assessment of dispersion of ceramic powders in organic vehicle. Ideally, the assessment involves two phases: a mixing operation wherein shear stress can be evaluated and controlled, and a quick and reliable method to examine the state of dispersion of the powder.

Although modern mixing machines such as the twin-screw extruder or double-lobed rotor mixer have taken over most compounding work, shear flow in such machines is too complicated to be evaluated. Such devices incorporate many complex flow paths.⁴ An attractive feature of the twin-roll mill, on the other hand, is its geometrical simplicity which permits the evaluation and control of the maximum shear stress set up in the mixture.

A number of methods have been developed for the assessment of dispersion of pigments or mineral fillers in polymers and rubbers. In contact micro-radiography (CMR), a thin slice of sample is placed in contact with a fine-grained photographic emulsion and exposed to X-rays. The resulting image is

either examined microscopically or enlarged photographically.⁵ In the thin film test, a suspension is heated and biaxially stretched by free blowing into a thin film bubble. Illumination inside the bubble shows up the undispersed agglomerates.⁵ In the extruder screen pack plugging test,⁶ an extruder is fitted with a series of screen packs which can vary in number and mesh size. The agglomerates caught on the screen after extrusion can then be examined.

These techniques are subject to difficulties when applied to assessing crowded suspensions for injection moulding of fine ceramic powders. Firstly, high powder volume fraction would make it difficult either to form thin films which are light transparent or to use screen packs. Secondly, the assessment of dispersion of ceramic powders in the sub-micron region requires high magnification and resolution which limits the use of low magnification visual methods such as illuminated thin film or CMR.

Methods based on the separation of powders from the matrix are available. A suspension can be ashed and the remaining powder examined microscopically. Organic vehicle may be dissolved with solvent so that the liquid-like diluted suspensions can be assessed using the methods for paint and ink industries (e.g. light scattering or the Coulter counter techniques^{7,8}). The dispersion state of a powder, however, is likely to change during the separation processes either by solid bridge agglomeration formed on ashing or by flocculation occurring on dilution in an added solvent.

Transmission electron microscopy (TEM) may reveal clearly the details of individual particles. But there are considerable difficulties in the preparation of electron-transparent thin films from a suspension. The overlapping images of particles or agglomerates may also cause difficulty in the interpretation of the results.

In scanning electron microscopy (SEM), dispersion is examined according to the information from a sectioned surface of a sample. If the secondary electron image is collected, the sample surface may have to be etched by solvent or ion bombardment⁹ in order to reveal the undispersed agglomerates. The back-scattered electron image technique (BEI) has been used to assess the dispersion in ceramic composites¹⁰ because phase contrast may be greatly enhanced as a result of atomic number difference.

Table 1. Materials used in this work and their sources

<i>Material</i>	<i>Grade</i>	<i>Manufacturer</i>
Spray-dried ZrO ₂ powder	Z1	Tioxide Specialties Ltd, UK
Spray-dried ZrO ₂ powder	SY-ULTRA(5.2)	Z-Tech, Australia
TiO ₂ pigment	RSM3	Tioxide Europe Ltd, UK
Polystyrene	HF555	BP Chemicals Ltd, UK

BEI analysis is based on the atomic number contrast and the back-scattering coefficient increases with increasing atomic number. This means that phases with higher atomic number constituents will be brighter than those containing only low atomic number elements. This work takes advantage of the fact that the atomic number in ceramic powders are normally much higher than those of the organic vehicle. Etching of samples is thus unnecessary. This reduces the sample preparation time and all that is required is a fractured surface of the solidified mixture; no polishing is needed.

In the present work the dispersion of a given powder is assessed with BEI in conjunction with quantitative twin-roll mill mixing.

2 Experimental Details

2.1 Materials

The materials used in this work and their sources are given in Table 1. The Z1 is an experimental grade of zirconia. The titania is an uncoated pigment precursor.

2.2 The twin-roll mill mixing

The twin-roll mill was 12 × 6 in model (Joseph Robinson & Co. Ltd, Manchester, UK). The roll speeds were 16.9 and 20.7 rpm. The roll length was 305 mm and the diameter was 152.4 mm. This gives surface speeds of 0.135 and 0.165 m s⁻¹, respectively. The rolls were heated with oil supplied by an electric immersion heater (Churchill Instrument Co. Ltd, Middlesex, UK). The temperature in the mixture was measured with a type K thermocouple probe during interruption to roll rotation. The polystyrene was melted on the rolls and then powder was added in stages. Mixing was performed at each temperature for approximately 30 min and during this period material was frequently removed and folded to enhance the lateral mixing. The typical sample volume was about 150 × 10⁻⁶ m³ so that with an average speed of 0.15 m s⁻¹ through a nip of 0.2 mm, each element of material passed the nip approximately 100 times giving it sufficient opportunity to be subject to the maximum shear stress.

2.3 Assessment of dispersion using the BEI technique

The mixed suspensions were granulated and compression moulded to discs of about 3 mm thick. These discs were then broken and the fractured surface was coated by carbon evaporation. The samples were examined with a JEOL JXA-840A SEM using the BEI mode. A slow scanning speed, 20 kV activation voltage, 10–15 mm working distance and a 10⁻⁶ to 10⁻⁷ A beam current were used to obtain satisfactory images.

Table 2. Variation of apparent viscosity of HF555 (Pa.s) with the temperature and shear rate

Shear rate (s ⁻¹)	Temperature (°C)			
	146	165	187	207
13	6130	—	—	—
26	5200	2530	1190	—
52	3760	1680	817	460
105	2970	1071	544	320
522	—	334	167	90
1044	—	219	108	67
1567	—	—	84	—

2.4 Capillary rheometry

Polystyrene HF555 was twin-roll milled at 168°C for 20 min to simulate the thermomechanical experience of the suspensions and its viscosity was tested using an Extrusion Rheometer (Davenport Ltd, London UK). The capillary was 2.10 mm in diameter and 40 mm in length. The tests were carried out at a range of temperatures and shear rates as shown in Table 2. Mixed suspensions were also tested in the same way to obtain the viscosity variation and the swell ratio β was found from the diameters of the capillary and the extrudate.

3 Results and Discussion

3.1 Quantitative dispersive mixing

Knowledge of the apparent viscosity of the suspension combined with the geometry and speeds of the mill allow calculation of the maximum shear stress experienced by the melt as it passes the nip. Since the mill rolls advance at different speeds, the maximum shear rate can be found from the following equations developed by Cogswell¹¹ based on McKelvey's work on shear rate distribution in the nip.¹²

$$\dot{\gamma}_{\max} = \dot{\gamma}_1 + \dot{\gamma}_2 \quad (1)$$

where

$$\dot{\gamma}_1 = \frac{3v}{H_0} \frac{1}{4(1 + \lambda^2)} \quad (2)$$

or

$$\dot{\gamma}_1 = \frac{3v\lambda^2}{H_0} \quad (3)$$

whichever is the larger, and

$$\dot{\gamma}_2 = \frac{v_2 - v_1}{2H_0} \quad (4)$$

where v_1 and v_2 are the surface speeds of the rolls and v is the average speed; H_0 is half the minimum gap between the rolls as shown in Fig. 1 which can be

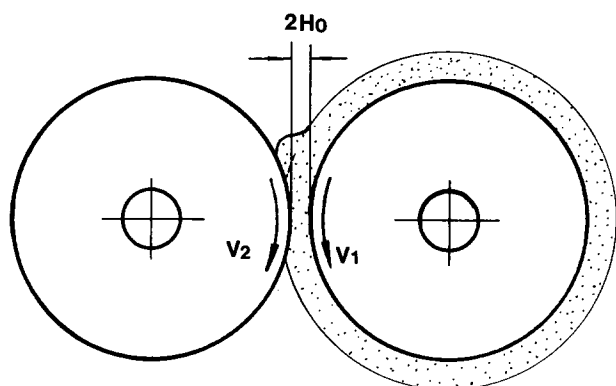


Fig. 1. Geometry of the twin-roll mill.

found with slip gauges; the parameter λ is related to the swelling ratio of the material (β) and can be calculated from

$$\lambda^2 = \beta - 1 \quad (5)$$

β can be estimated from change in diameter in the capillary rheometry test discussed below. These equations are slightly simpler than similar expressions developed by Tadmor and Gogos.¹³

The maximum shear stress can be found from eqn (6):

$$\tau_{\max} = \eta \dot{\gamma}_{\max} \quad (6)$$

where η is the apparent viscosity of the suspension at $\dot{\gamma}_{\max}$ and the given mixing temperature (T). Equations (1)–(6) show that the shear stress in a twin-roll mill can be controlled by adjusting the roll speeds, the gap between the rolls and the temperature of mixing.

For a given organic vehicle at a fixed volume fraction, the relationship

$$\eta = \eta(\dot{\gamma}, T) \quad (7)$$

can be obtained from rheometry. Figures 2 and 3

show the variation of apparent viscosity (η) with the mixing temperature (T) and the shear rate ($\dot{\gamma}$) for the polystyrene used in this work.

The following equations¹⁴ can be used to generalise the data in Fig. 2:

$$\eta = A e^{(E/RT)} \quad (8)$$

Here, R is the gas constant and A is a material constant; E is sometimes denoted activation energy. Although the use of an activation energy to express the temperature dependence of viscosity has met with considerable opposition on the grounds of its physical meaning,¹⁵ the equation allows viscosity to be found over a range of temperature from a small number of experimental results. The parameters in eqn (7) are given in Table 3. Similarly, the data in Fig. 4 can be expressed by the equation for a power law fluid:

$$\eta = K \dot{\gamma}^{n-1} \quad (9)$$

which can be rewritten as

$$\log \eta = (n-1) \log \dot{\gamma} + \log K \quad (10)$$

where the flow behaviour index n and the constant $\log K$ are shown in Table 4.

When powders are added to an organic vehicle, the viscosity increases with the volume fraction, V . Viscosity of the suspension with 10 vol% RSM3 at 168°C showed that relative viscosity η/η_0 obeys the Einstein equation:

$$\frac{\eta}{\eta_0} = 1 + 2.5V \quad (11)$$

irrespective of shear rate (Fig. 4). This is generally the case for diverse powders in the $V < 0.1$ region. The problem of fitting relative viscosity to idealised equations occurs at high V . This allows the viscosity

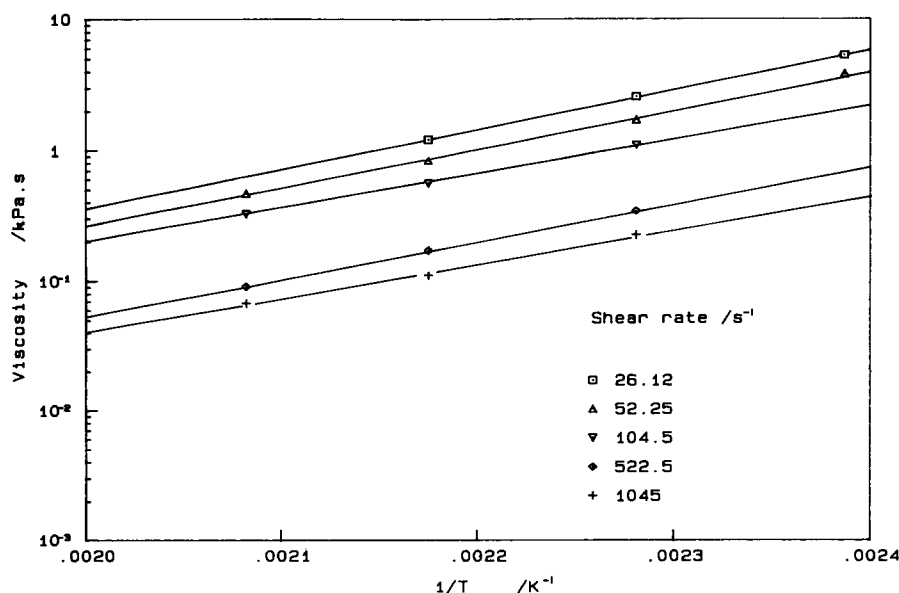


Fig. 2. Variation of the apparent viscosity of HF555 polystyrene with temperature.

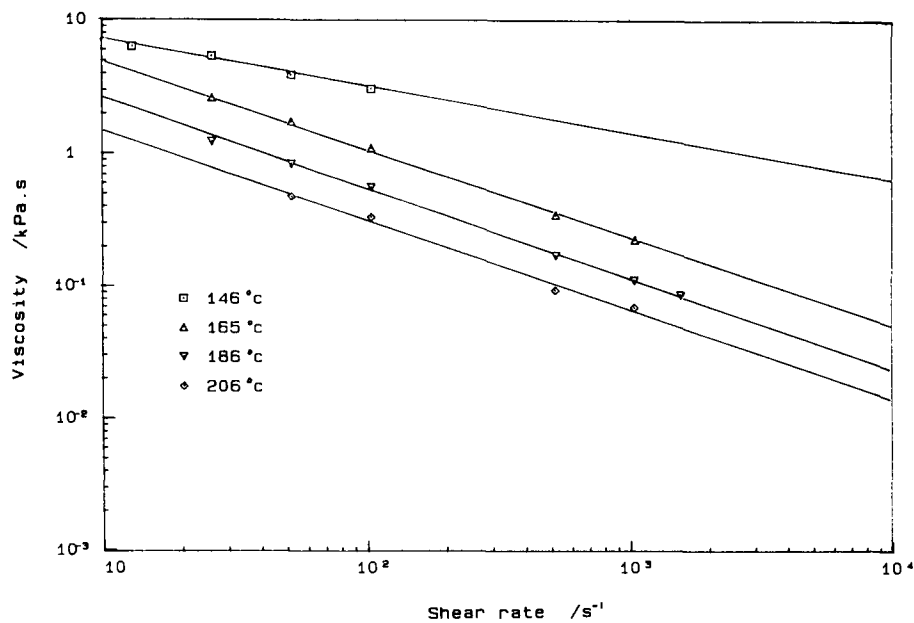


Fig. 3. Variation of the apparent viscosity of HF555 polystyrene with the shear rate.

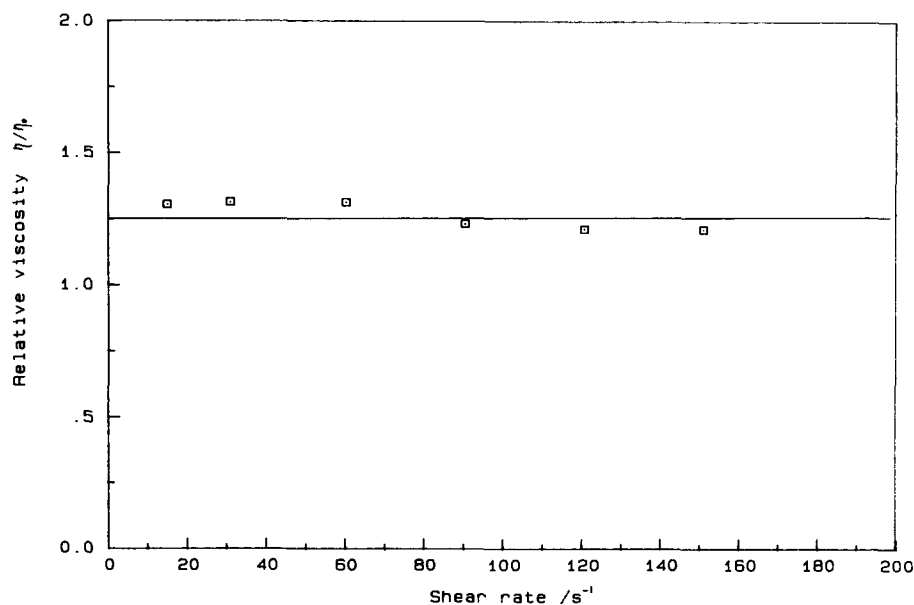


Fig. 4. The ratio of apparent viscosity of the suspension with 10 vol% RSM3 pigment (η) to that of the unfilled HF555 polystyrene (η_0) tested at 168°C as a function of shear rate.

of a suspension with 10% ceramic volume fraction to be found based on eqns (8), (9) and (11).

Thus, suspensions of approximately 10 vol% ceramic can be mixed with a twin-roll mill over a wide range of shear stress achieved by adjusting temperature or the gap between the rolls. The dispersion of a powder can then be tested under a chosen shear

stress. The procedure does not prevent the use of other materials as organic vehicle provided the relationships defined by eqns (8) and (9) are experimentally determined.

Unlike the dispersion of powders in low-viscosity organic liquids, polymeric organic vehicle usually cannot penetrate the agglomerates in real mixing times to affect the adhesion forces between the

Table 3. The constants in eqn (8)

Shear rate (s^{-1})	E ($kJ mol^{-1}$)	ln
26	57.8	-15
52	57.2	-15.2
105	56.0	-16.0
522	54.7	-16.2
1045	50.0	-15.2

Table 4. The constants in eqn (9)

Temperature (°C)	n	$log K$
146	0.653	4.11
165	0.324	4.37
186	0.335	4.04
207	0.324	4.83

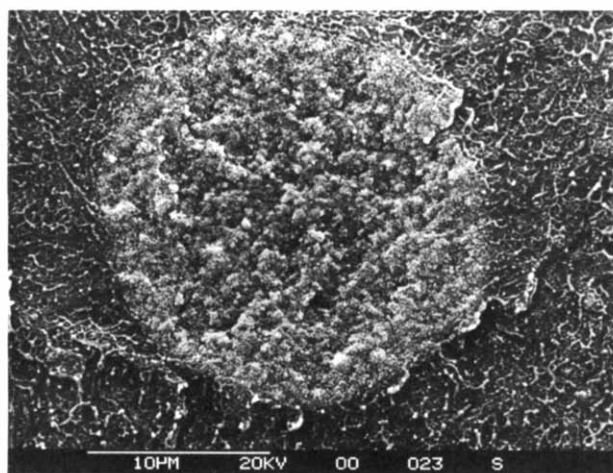


Fig. 5. An agglomerate of Z1 in HF555 polystyrene showing negligible penetration of polymer into the agglomerate.

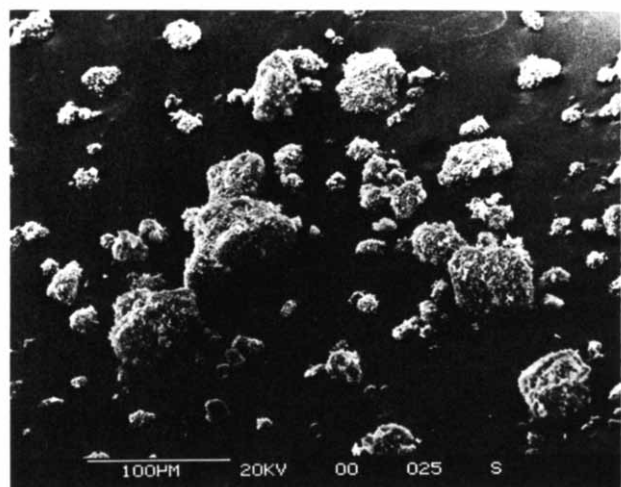
particles. An example is shown in Fig. 5 where the fracture surface of the agglomerate can be distinguished from the matrix and is characteristic of a powder assembly. Thus, the strength of agglomerates can be considered to be unchanged during mixing.

Two microscopic mechanisms of dispersion have

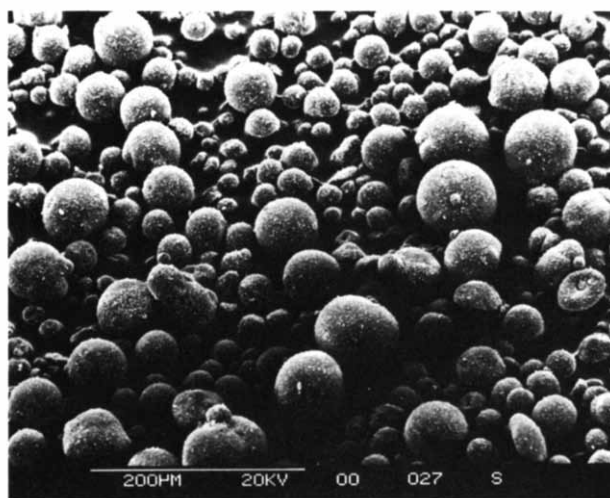
been suggested: erosion, where particles are washed away gradually from the agglomerates even under low shear stresses, or fracture where agglomerates break down when shear stress reaches their strength. The relative importance of the two mechanisms has rarely been established and may depend on the nature of the agglomeration. Observation of carbon black agglomerates breaking down in simple shear flow¹⁶ showed that erosion was a slow process and the agglomerate size remained virtually unchanged until the shear stress reached a critical value. This suggests that the dominant factor controlling dispersion in practice is the relationship between shear stress generated in the suspension and the agglomerate strength.

3.2 Assessment of dispersion

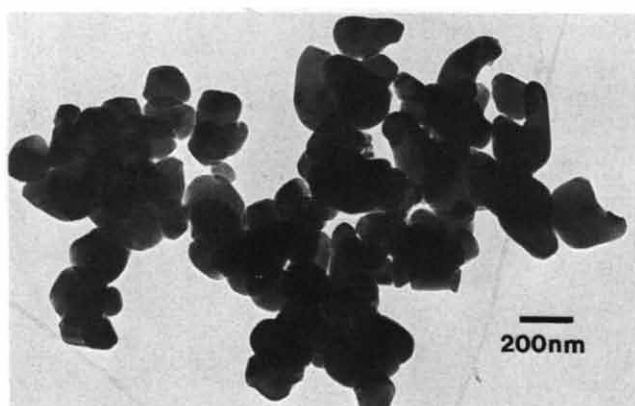
The powders in the as-received state are shown in Figs 6–8. These reveal the agglomerate shape and size distribution as shown by SEM and the ultimate particle shape and size as shown by TEM. The average particle size of the titania powder is approximately 0.2 μm and it is naturally agglomerated into a wide range of sizes of irregular



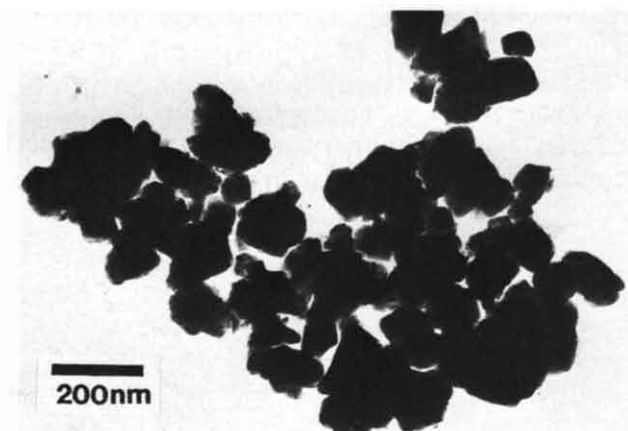
(a)



(a)



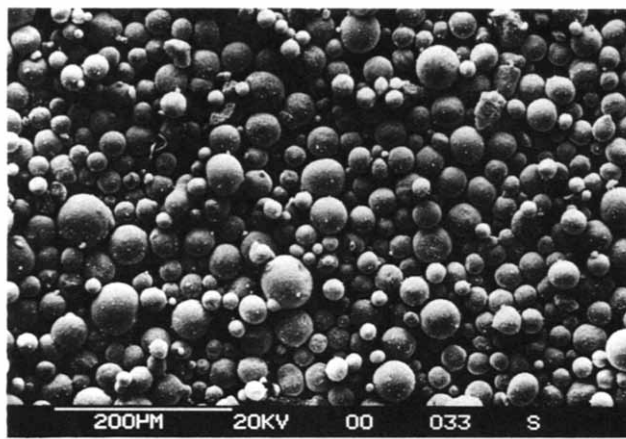
(b)



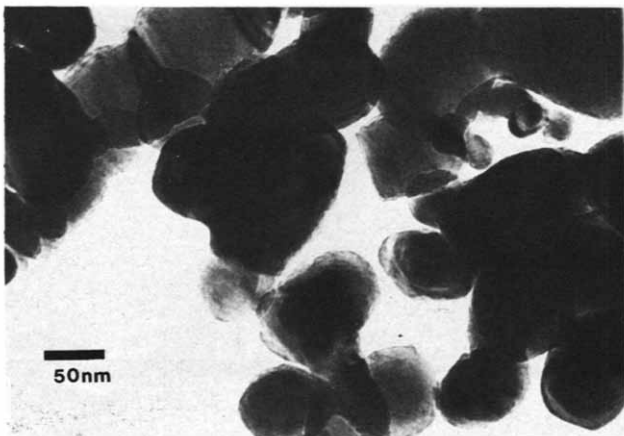
(b)

Fig. 6. (a) SEM of agglomerates, and (b) TEM of particles in RSM3 TiO₂ pigment.

Fig. 7. (a) SEM of agglomerates, and (b) TEM of particles in SY-ULTRA ZrO₂ powder with Y₂O₃ additions.



(a)



(b)

Fig. 8. (a) SEM of agglomerates, and (b) TEM of particles in Z1 ZrO₂ powder with Y₂O₃ additions.

shape. The particles of SY-ULTRA are irregularly shaped with an average size of 0.3 µm. It is spray-dried to give spherical agglomerates with an average diameter of 50 µm. The Z1 experimental powder has a smooth shape with diameters in the 50–100 nm region and has been spray dried to give agglomerates of 20 µm average diameter.

Suspensions with approximately 10 vol% ceramic are ideal for dispersion assessment using the BEI technique, and were used throughout. Generally, however, the volume fraction of suspensions for injection moulding are much higher (typically 45–60 vol% for sub-micrometre particles). Under such circumstances eqn (11) can no longer be used to

obtain the viscosity of the suspension and an expression for relative viscosity as a function of ceramic volume fraction which is valid for concentrated suspensions must be employed. To assess the dispersion of high ceramic fraction suspensions, the sample would have to be diluted to approximately 10 vol% ceramic after dispersive mixing.

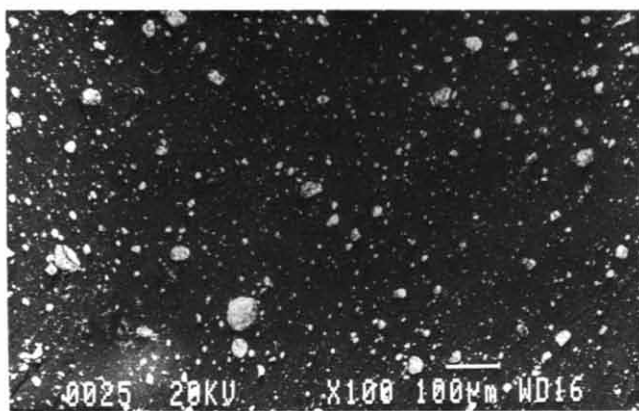
The assumption made here is that the dilution process, which includes an extra period of mixing, albeit at much reduced maximum shear stress because of the lower ceramic volume fraction, does not affect the state of dispersion. In order to verify this, the influence of mixing time was investigated. Two powders, SY-ULTRA and Z1, were mixed at 10 vol% with the polystyrene at the same mixing condition (see condition 2 in Table 5). Samples were taken off the rolls at 15, 20, 25 and 30 min. Shorter mixing times are impractical because of the need to achieve uniformity of composition on the rolls. The fracture surfaces were examined by the BEI technique and Figs 9 and 10 show that the backscattered electron images gave sharp contrast between the powder and organic vehicle. Only the 10 and 30 min mixing times are shown and are indistinguishable. This indicates that the effect of mixing time on the state of dispersion is insignificant at a fixed shear stress and therefore this assumption is reasonable.

Obtaining a fracture surface for BEI assessment is normally straightforward as discussed above. With softer organic vehicles such as those based on waxes, the sample can be fractured in liquid nitrogen. The essential requirement for obtaining a clear BEI is to use a high acceleration voltage, a slow scanning speed, a short working distance and sufficient beam current.

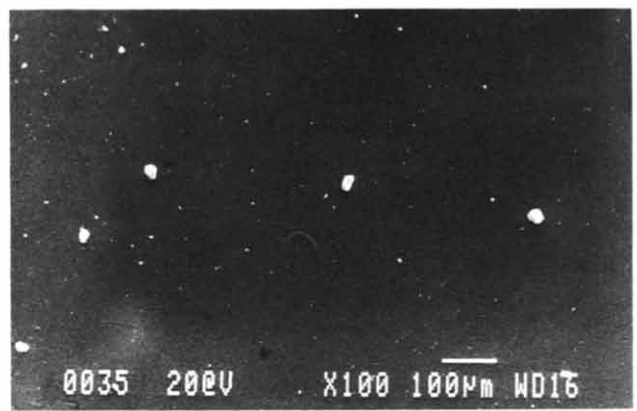
A method has been described for the assessment of average agglomerate strength using an instrumental uniaxial die pressing test.¹⁷ In this method, the deformation of the compact is plotted as a function of the logarithm of pressure so that the sharp discontinuity in the curve can be used to indicate a nominal critical pressure, p_c , at which agglomerates start to break down. By obtaining the area fraction of agglomerates involved in load transmission, the experimental value of p_c can be compared with the strength of agglomerates as measured by a single agglomerate strength testing

Table 5. The mixing conditions and maximum shear stresses

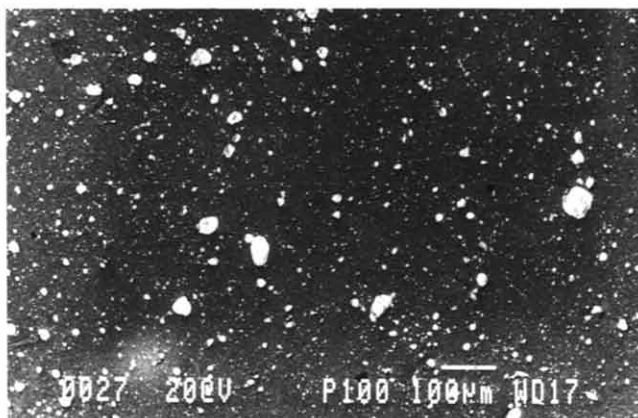
Condition	Powder	Temperature (°C)	Nip size, $2H_0$ (mm)	Mixing time (min)	Max shear stress (MPa)
1	RSM3 Z1	165	0.2	30	0.3
2	SY-ULTRA Z1	146	0.4	15, 20 25 and 30	1.8



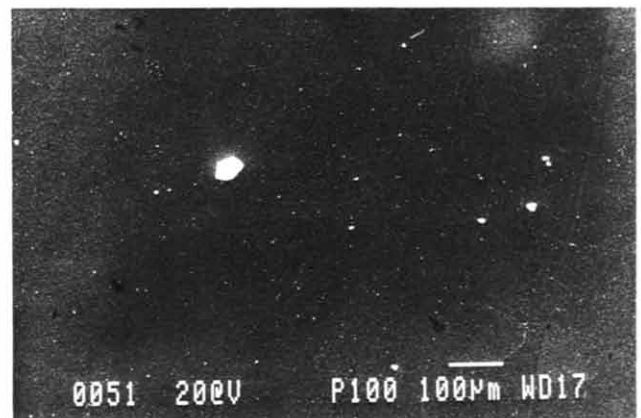
(a)



(a)



(b)



(b)

Fig. 9. Dispersion states of Z1 in HF555 polystyrene mixed under a maximum shear stress of 1.8 MPa (condition 2 shown in Table 5) for (a) 15 min, and (b) 30 min.

Fig. 10. Dispersion states of SY-ULTRA in HF555 polystyrene mixed under a maximum shear stress of 1.8 MPa (condition 2 shown in Table 5) for (a) 15 min, and (b) 30 min.

method.¹⁷ For spherical agglomerates, the tensile strength σ is estimated as

$$\sigma \approx 0.52p_c \quad (12)$$

This test was applied to the powders studied here and the results are shown in Fig. 11. The nominal critical pressure p_c was found to be 0.05 MPa for RSM3 and 0.23 MPa for SY-ULTRA. In the test for Z1, no sharp discontinuity was found in the pressure–deformation curve therefore a single value of p_c could not be clearly identified (Fig. 11(c)). This suggests that the agglomerate strength distribution is wide and agglomerates tend to deform at widely different pressures. This is confirmed by fracture surfaces of the samples after compaction up to 10 MPa. For the low agglomerate strength SY-ULTRA, the relics of agglomerates are visible in the fracture surface which is typical of pressed unfired ceramic assemblies. The relics are faceted and shape-accommodation is presented. On the other hand, unfaceted agglomerates surrounded by a well-compacted powder matrix were observed within the sample of Z1 (Fig. 12(b)). There is little evidence here of shape-accommodation. These agglomerates have apparently resisted deformation.

The next stage of this work is to test dispersion

using the twin-roll mill and BEI in the light of estimations of agglomerate strength. The states of dispersion for the powders studied are shown in Figs 9, 10, 13 and 14. The penetration depth of the electron beam was approximately $1 \mu\text{m}$ so the image includes the sub-micrometre particles within this depth. The undispersed agglomerates and the well-dispersed particles can clearly be observed by varying the magnification. In agreement with the die pressing agglomerate strength measurement, RSM3 disperses well (Fig. 13). A few residual agglomerates in the $1 \mu\text{m}$ region (5 particle diameters) are visible. For most high strength ceramic applications, a defect size in the $1 \mu\text{m}$ region is more than acceptable. It is noticeable that this excellent state of dispersion is obtained from a powder specially designed for mixing with organic media in paint and printing ink applications. The RSM3 with $p_c = 0.05$ MPa has, according to the calculation described above, been subject to a maximum shear stress in mixing of 0.3 MPa, which is 11 times as high as the agglomerate tensile strength if eqn (12) is used. Even at this high ratio of applied stress to tensile strength, some undispersed agglomerates remain.

The dispersion of SY-ULTRA after mixing with a maximum shear stress of 1.8 MPa is shown in Fig.

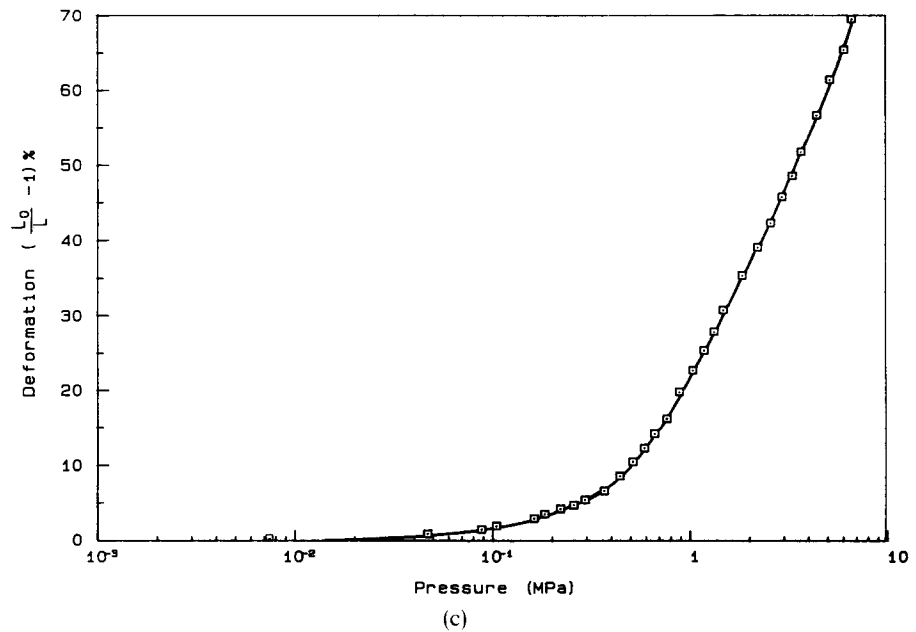
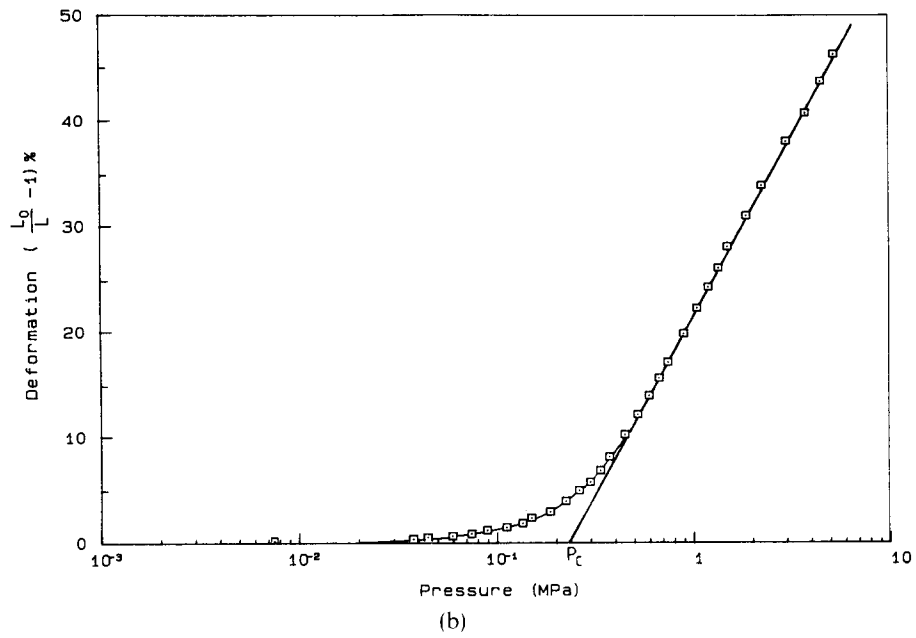
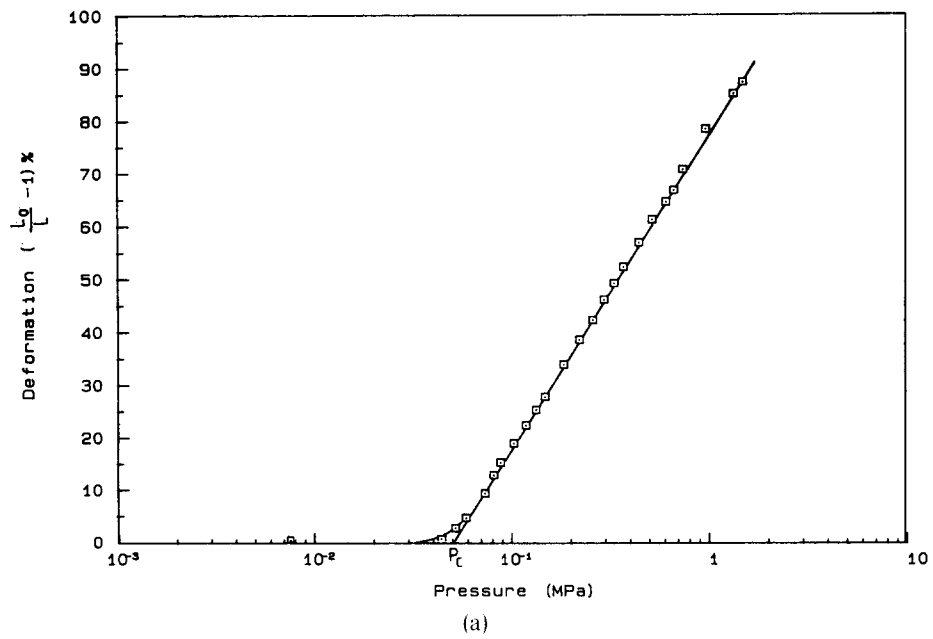
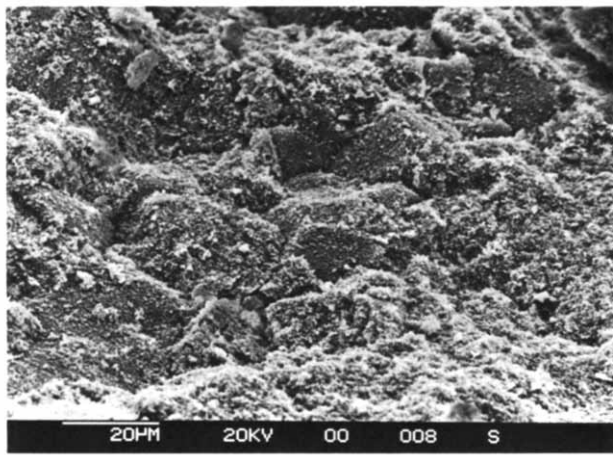
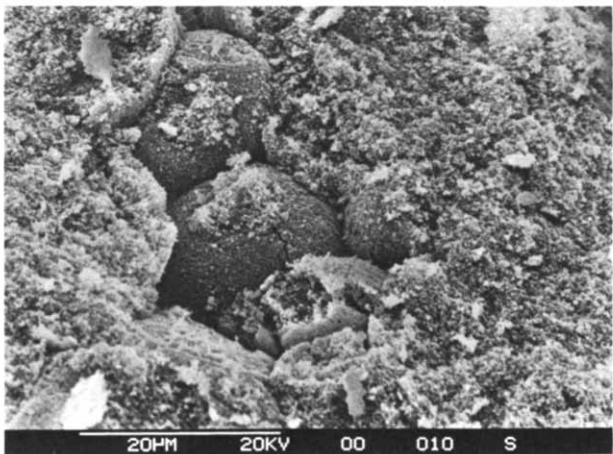


Fig. 11. Die pressing tests where l_0 and l are the sample height before and during pressing. (a) RSM3, (b) SY-ULTRA, and (c) Z1.



(a)

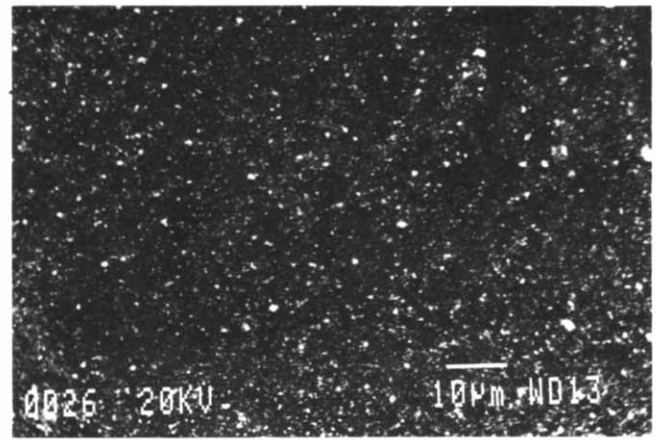


(b)

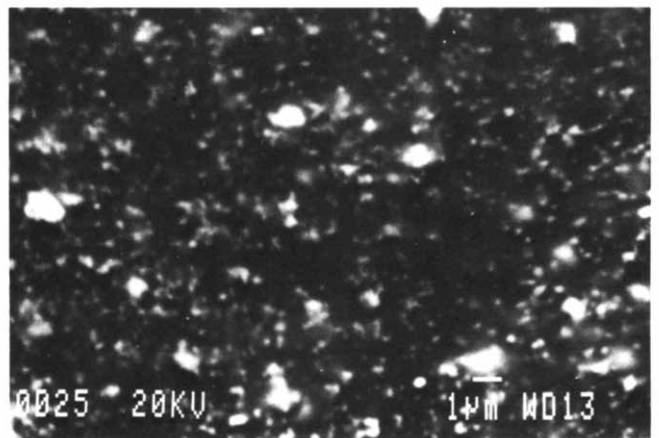
Fig. 12. SEM of fractured surface of pressed assemblies uniaxially compacted to 10 MPa. (a) SY-ULTRA, and (b) Z1.

10. The powder has a p_c of 0.24 MPa, equivalent to a tensile strength of 0.12 MPa. The maximum shear stress imposed therefore is about 14 times as high as the tensile strength. Like the RSM3, the mixing has been effective but in this case, a small population of large particle assemblies remain. It is interesting to note that these are not spherical in shape. They are in fact the fractured pieces from the original agglomerates.

Figures 9 and 14 show the dispersion of Z1 at two different maximum shear stresses, 1.8 and 0.3 MPa, respectively. A single value for p_c cannot be deduced as discussed above, but if an extrapolation were attempted, p_c would be in region 0.4–0.7 MPa. The low stress mixing condition (Fig. 14), where the maximum shear stress (0.3 MPa) is within the region of the tensile strength (0.22–0.38 MPa), shows sections of spherical agglomerates in the fracture plane. Very little agglomerate fracture has taken place as witnessed by the sphericity. In contrast, mixing under a high shear stress of 1.8 MPa (Fig. 9), where the maximum shear stress is between five and eight times as high as the estimate of tensile stress, has produced considerable agglomerate damage.



(a)

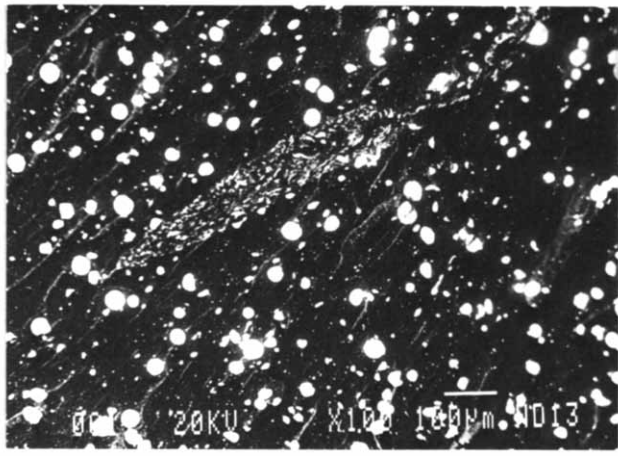


(b)

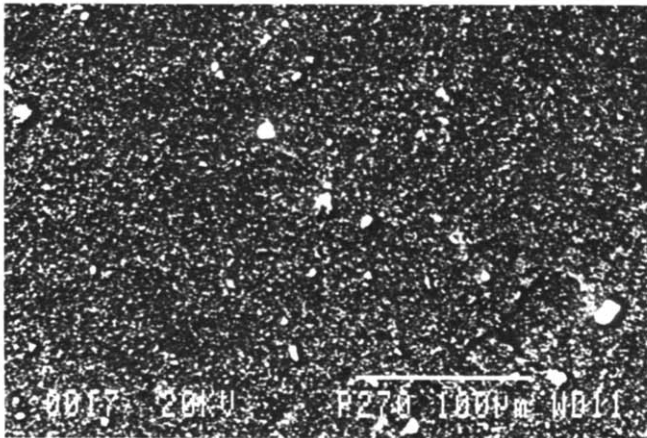
Fig. 13. Dispersion of RSM3 pigment in HF555 polystyrene mixed under a maximum shear stress of 0.3 MPa (condition 1 shown in Table 5): (a) low magnification, and (b) high magnification.

The fracture debris is irregular in shape and the size distribution has widened. This also indicates the existence of very strong agglomerates and the wide distribution of agglomerate strength as discussed above. Comparison of Figs 9(a), 9(b) and 14 clearly show that agglomerate rupture is a function of maximum applied shear stress during mixing rather than mixing time.

It is interesting to note that a high ratio of imposed maximum shear stress to the estimated agglomerate tensile strength must be used to achieve effective dispersive mixing. In contrast, Rwei *et al.*¹⁶ working with carbon black agglomerates, appear to show that the shear stress needed for dispersion was generally less than the tensile strength of agglomerates. However, the tensile strength was measured on compacted agglomerates while the dispersion experiments were performed on pellets made by wetting, tumbling and drying and this complicates the interpretation. Furthermore, their agglomerate strength was found to be affected by the penetration of liquid. Thus although 50 wt% of the agglomerates had been reduced to submicrometre aggregates



(a)



(b)

Fig. 14. Dispersion of Z1 powder in HF555 mixed under a maximum shear stress of 0.3 MPa (condition 1 shown in Table 5): (a) low magnification, and (b) high magnification.

when the ratio of applied shear stress to measured tensile strength was unity, the tensile strength upon which this ratio is based was some 26 times the agglomerate strength estimated from rupture visualisation in their cone and plate rheometer. Their results are therefore consistent with the results reported here.

A further complication is the influence of hydrostatic stress on agglomerate failure stress in shear flow. Significant hydrostatic stress can be developed in mixing machinery particularly in twin-screw extrusion where the chamber pressure could rise to 20 MPa or more. In the twin-roll mill, hydrostatic stress is much less but may still increase the agglomerate failure stress in a shear mode τ_f . The Mohr–Coulomb failure criterion for the particle assembly within an agglomerate can be expressed as

$$\tau_f = \sigma_n \tan(\phi_f) + c \quad (13)$$

where σ_n is the normal stress on the failure plane which is equal to the hydrostatic stress in the suspension, c is the cohesive shear strength of the agglomerate at zero pressure; ϕ_f is the peak angle of internal friction and it is related to the packing of

particles and the friction coefficient between them.¹⁸ An estimate can be made using Jacky's equation¹⁸

$$\sin(\phi_f) = 1 - K_0 \quad (14)$$

where K_0 is the ratio of lateral to axial stress in uniaxial compaction. Taking a typical value of $K_0 = 0.4$ for ceramic powders,¹⁹ then $\tan(\phi_f) = 0.75$. This means the effective agglomerate strength will always rise with applied pressure.

Agglomerate strength depends very much on the size of defects resulting from the heterogeneities in packing within agglomerates and according to Kendall²⁰ is given by

$$\sigma = 15.6\phi^4\Gamma_c^{5/6}\Gamma^{1/6}(d_0C)^{-1.2} \quad (15)$$

where C is the critical defect size in the agglomerate; d_0 is the particle diameter; ϕ is the packing efficiency of particles in the agglomerate; Γ_c is the interfacial energy between particles; and Γ is the measured fracture energy. Thus, experimental measurement of agglomerate strength represents the lowest shear stress needed to break the original agglomerates. Successively higher shear stresses must be imposed in order to fracture the debris broken from the original agglomerates. This arises because of the dependence of critical flaw size on volume and can be illustrated by the following somewhat simplified treatment.

The average strength σ_1 , of agglomerates of volume V_1 is related to the average strength σ_2 of agglomerates of volume V_2 by the Weibull modulus m :

$$\frac{\sigma_1}{\sigma_2} = \left(\frac{V_2}{V_1}\right)^{1/m} \quad (16)$$

Assuming that each successive fracture halves the size of agglomerate fragments, the strength after n fractures is

$$\sigma_{n+1} = \sigma_1 \left(\frac{1}{2}\right)^{-n/m} \quad (17)$$

To reduce the volume of an agglomerate to 1/1000 of its original volume requires approximately 10 fractures. The final strength would then be ten times the original strength if the agglomerates are awarded a rather generous Weibull modulus of 3, Kendall and Weihs²¹ record a Weibull modulus of 1.5 on spray-dried zirconia agglomerates. An inferior Weibull modulus would produce a greater climb in agglomerate strength.

4 Conclusions

A method has been developed for the assessment of dispersive mixing of ceramic powder in organic vehicle for injection moulding and related processes. The maximum shear stress imposed in a suspension

during mixing can be calculated based on the geometry of a twin-roll mill and the rheological properties of the selected organic vehicle. The corresponding dispersion state can be assessed with backscattered electron image techniques on an SEM.

The BEI dispersion assessment method can be used on its own as a quick assessment of dispersion of powder or other filler in organic materials. Highly filled suspensions need to be diluted in order to reveal clearly the dispersion state. This can easily be achieved in practice. By studying three diverse powders, the agglomerate tensile strength deduced from nominal critical pressure, p_c in an experimental die pressing test can be used as a guide for mixing conditions. The maximum shear stress imposed during mixing should at least exceed the tensile strength to break the original agglomerates but it must be considerably higher than the measured agglomerate tensile strength to achieve effective dispersive mixing. This is attributed to the increase of the effective strength of agglomerates (or debris) as a result of hydrostatic stress imposed in the suspension during mixing and the reduction of flaw size in the debris broken from the original agglomerates.

The examples in this work showed that the dispersive mixing of agglomerated powder in organic vehicle is dominated by the agglomerate strength and the shear stress imposed in the suspension during mixing. Mixing time is found to be less important.

Acknowledgements

The authors are grateful to the Science and Engineering Research Council and the Link Nanotechnology Scheme for supporting this work. Dr G. Dransfield at Tioxide Chemicals, UK is thanked for helpful discussions and the supply of the powders.

References

1. Rumpf, H. & Schubert, H., Adhesion forces in agglomeration processes. In *Ceramic Processing before Firing*, ed. G. Y. Onoda Jr & L. L. Hench. Wiley Interscience, New York, USA, 1978, pp. 357–77.
2. Lange, F. F. & Metcalf, M., Processing related fracture origins: II Agglomerate motion and cracklike internal surface caused by differential sintering. *J. Am. Ceram. Soc.*, **66** (1983) 398–406.
3. Lange, F. F. & Davis, B. I., Processing related fracture origins: III Differential sintering of ZrO₂ agglomerates in Al₂O₃/ZrO₂ composite. *J. Am. Ceram. Soc.*, **66** (1983) 407–8.
4. Martelli, F. G., *Twin Screw Extruders*. Van Nostrand, New York, USA, 1983, p. 75.
5. Ess, J. W., Hornsby, P. R., Lin, S. Y. & Bevis, M. J., Characterisation of dispersion in mineral-filled thermal-plastics compounds. *Plast. Rubb. Proc. Applic.*, **4** (1984) 7–14.
6. Gagné, B. A., Titanium dioxide pigments in plastics. TiNFO system. Ti oxide, London, 1989, pp. 11–13.
7. Richards, L. W., Size distribution of pigment particles. In *Pigment Handbook* (Vol. 3), ed. T. C. Patton. John Wiley and Sons, London, UK, 1973, pp. 89–100.
8. Bell, S. H. & Crowl, V. T., Assessment of the state of dispersion. In *Dispersion of Powders in Liquids* (2nd edn), ed. G. D. Parfitt. Applied Science Publishers, London, UK, 1973, pp. 267–307.
9. Prasser, J., Plasma etching of paint films to examine pigment dispersion. *Polym. Paint. Colour J.*, **175** (1985) 390–2.
10. Zhang, J. G., Edrington, M. J. & Evans, J. R. G., On the dispersion of unary and binary ceramic powders in polymer blends. *Proc. Br. Ceram. Soc.*, **42** (1989) 91–9.
11. Cogswell, F. N., The rheological experience of PVC melt in a calendar nip. Conference paper in *Journée Calendrage, Papiers d'une Réunion, Groupe Français d'Études et d'Application des Polymères, Section Lyonnaise*, ed. J. Nivière. Lyon, 1975, p. 6.
12. McKelvey, J. M., *Polymer Processing*. Wiley, New York, USA, 1962, pp. 211–27.
13. Tadmor, Z. & Gogos, C. G., *Principles of Polymer Processing*. Wiley, New York, USA, 1979, pp. 442–7.
14. Patfoort, G. A., *Polymers, An Introduction to Their Physical and Rheological Behaviour*. Scientific Publishers, Belgium, 1974, p. 174.
15. Hildebrand, J. H., Operations on swollen theories with Occam's razor. In *Structure–Property Relationship in Polymers*, ed. F. W. Harris & R. B. Seymour. Academic Press, New York, USA, 1977, pp. 1–10.
16. Rwei, S. P., Manas-Zloczower, I. & Feke, D. L., Observation of carbon black agglomerate dispersion in simple shear flows. *Polym. Engng. Sci.*, **30** (1990) 701–6.
17. Song, J. H. & Evans, J. R. G., A die pressing test for estimation of agglomerate strength, to be published.
18. Fedá, J., *Mechanics of Particulate Materials, the Principles*. Elsevier Scientific Publishing Company, Amsterdam, The Netherlands, 1982, pp. 153–75.
19. Song, J. H. & Chandler, H. W., Determination of some compaction properties of ceramic powders using a simple cylindrical apparatus. *Br. Ceram. Trans. J.*, **89** (1990) 49–52.
20. Kendall, K., Agglomerate strength. *Powder Metall.*, **31** (1988) 28–31.
21. Kendall, K. & Weihs, T. P., Adhesion of nanoparticles within spray-dried agglomerates. *J. Phys. D. Appl. Phys.*, **25** (1992) A3–A8.